Article

Short-Term Exposure to PM_{10} and Black Carbon in Residential Microenvironments in Bragança, Portugal: A Case Study in Bedrooms, Living Rooms, and Kitchens

Yago Alonso Cipoli [1,2,3,*], Carla Alexandra Gamelas [4,5], Susana Marta Almeida [4], Manuel Feliciano [2,3] and Célia Alves [1,*]

1 Centre for Environmental and Marine Studies (CESAM), Department of Environment, University of Aveiro, 3810-193 Aveiro, Portugal

2 Centro de Investigação de Montanha (CIMO), Instituto Politécnico de Bragança, 5300-253 Bragança, Portugal; msabenca@ipb.pt

3 Laboratório Associado para a Sustentabilidade e Tecnologia em Regiões de Montanha (SusTEC), Instituto Politécnico de Bragança, 5300-253 Bragança, Portugal

4 Centro de Ciências e Tecnologias Nucleares, Instituto Superior Técnico, Universidade de Lisboa, Estrada Nacional 10, 2695-066 Bobadela, Portugal; carla.gamelas@ctn.tecnico.ulisboa.pt (C.A.G.); smarta@ctn.tecnico.ulisboa.pt (S.M.A.)

5 Instituto Politécnico de Setúbal, Escola Superior de Tecnologia de Setúbal, Centro de Investigação em Energia e Ambiente, IPS Campus, 2914-508 Setúbal, Portugal

* Correspondence: yagocipoli@ua.pt (Y.A.C.); celia.alves@ua.pt (C.A.); Tel.: +351-932111652 (Y.A.C.)

Abstract: Several studies have evaluated PM concentrations in single specific microenvironments as a measure of exposure in the entire house. In this study, PM_{10} was monitored at the same time in three microenvironments (bedroom, living room, and kitchen) from three dwellings located in a small inland town of the Iberian Peninsula to assess whether exposure varies significantly between them. Real-time optical instruments and low-volume gravimetric samplers were employed. A multi-wavelength absorption instrument was used to determine black carbon (BC) concentrations on the filters. The Multiple-Path Particle Dosimetry Model (MPPD) was applied to evaluate the deposition of PM_{10} and BC in the airways of adults. For all dwellings, the highest PM_{10} concentrations were recorded in bedrooms (B1 = 22.7 µg m^{-3}; B2 = 19.5 µg m^{-3}; and B3 = 68.1 µg m^{-3}). Houses 1 and 3 did not show significant differences between microenvironments. This did not happen in house 2, suggesting that ventilation is a determining factor for concentrations. BC originated mainly from fossil fuel emissions (90%), while biomass burning represented a minor contribution (10%). MPPD showed that PM_{10} is predominantly deposited in the head region ($\geq$85% of the total dose), while BC is mainly deposited in the pulmonary region (14%). Higher doses were estimated for males than for females.

Keywords: dwellings; microenvironments; PM_{10}; BC; dose; MPPD

1. Introduction

Air pollution has become a growing public health concern, especially in indoor environments, where people spend most of their time [1–3]. Scientific evidence has shown that inhalation of polluted air is associated with increased mortality and morbidity rates [4,5], reduced lung function [6,7], worsening of cardiorespiratory diseases [8,9], and cancer [10], even at low doses and short-term exposures. The World Health Organization (WHO) has estimated that a total of 3.2 million deaths per year worldwide are attributable to exposure to particulate matter (PM) in domestic environments [11]. PM is classified as a group 1 carcinogen and ranks fifth on the list of global death factors [12,13]. PM is a complex mixture of solid and liquid particles suspended in the air, varying in shape, aerodynamic diameter, and chemical composition, depending on the sources or formation processes [14].

The assessment and management of outdoor air quality are well-documented, with legally stipulated limit values in European countries. However, indoor air quality is regulated only in some countries (e.g., Portugal, Finland, Slovenia, and Lithuania). Rapid urbanisation contributes to changes in the lifestyle and habits of the population, with residents spending more than 90% of their time indoors, most of which is in homes [15]. Furthermore, indoor PM concentrations and chemical composition can be very distinct from those observed outdoors [16–18], with higher levels of PM and specific elements reported for indoor environments [19]. Thus, it is equally or even more important to assess PM inhalation and deposition in the human respiratory tract in these environments. In general, indoor PM concentrations are influenced by human activities, including emission sources such as cooking [20], smoking [21], heating systems [22], and particle resuspension [23], as well as residential characteristics, such as distance from external sources, orientation and layout, ventilation rates, air infiltration, and building materials [24–26].

Several studies have documented PM concentrations in specific microenvironments in dwellings, including living rooms, bedrooms, and kitchens [27–32]. Due to the noise generated by gravimetric instruments, few studies have evaluated these microenvironments simultaneously using reference methods. In general, the characterisation of dwellings is based on a single microenvironment using low-cost and/or photometric devices, which generate less discomfort for residents. However, the unavailability of a reference method simultaneous with other devices makes data interpretation difficult, since the aerosol composition can be different for each microenvironment. Thus, the present study focuses on monitoring PM_{10} concentrations in three different microenvironments (bedroom, living room, and kitchen) simultaneously, using optical and gravimetric equipment, to assess whether concentrations measured in one room are representative of exposures in other spaces of the house. In addition, Multiple-Path Particle Dosimetry (MPPD) was applied to evaluate the PM_{10} and BC deposition in the human respiratory tract for each microenvironment. The study can provide important information for directing future research in indoor microenvironments in dwellings and human health assessments.

2. Materials and Methods

2.1. Monitoring Sites

An indoor monitoring campaign in specific microenvironments (bedroom—B, living room—LR, and kitchen—K) was conducted in three naturally ventilated dwellings (Figure 1) in the city of Bragança. With a population of about 35,000 inhabitants [33], Bragança is located in the northeast of Portugal in a mountainous region (alt. 690 m), with a temperate climate (Csa) according the Köppen–Geiger classification [34]. The climate of the region is characterised by high thermal amplitude, with dry and hot summers and frequent rains in winter [35].

Figure 1. Location of the monitoring sites in the city of Bragança: (1) house 1, (2) house 2, and (3) house 3.

Given the annoying noise of the equipment, especially in the bedroom, the three target homes were selected from among the few residents who volunteered to participate in the study. The different configurations of each microenvironment are described in Table 1.

Table 1. Characteristics of dwellings and specific microenvironments.

Characteristics	House 1			House 2			House 3		
	B	**LR**	**K**	**B**	**LR**	**K**	**B**	**LR**	**K**
Location	Residential area			High-density traffic avenue			Apartment building/complex		
Orientation	Yard	Street	Street	Street	Yard	Yard	Parking	Parking	Street
Area (m^2)	16	30	30	12	20	10	10	40	20
Ventilation settings	CDSW *	ODSW *	ODOW *	CDSW *	CDCW *	CDCW *	CDSW *	ODOW *	ODCW *
Permanent occupants	4			3			4		
Daily occupancy (h)	20			14			24		
Pets	2 cats			No			1 dog		
Source of energy for cooking	Gas			Gas			Gas		
Apartment floor	1			1			3		

* OD/CD—open doors/closed doors; OW/SW/CW—open windows/semi-open windows/closed windows.

The selected houses were occupied by non-smoker students aged between 25–30 years. Students in Bragança represent 1/3 of the total population. During the sampling campaign, a logbook was left in each microenvironment so that the occupants of the residence could opportunely write down the activities developed there. Volunteers were requested to carry out activities under normal conditions. It is worth mentioning that, even though no heating system was used during the monitoring period, house 1 has an open fireplace, which may affect the ventilation rates of this environment. None of the houses had open spaces, that is, all microenvironments were individual rooms, communicating with each other through hallways. The average distance between microenvironments was 7 m.

2.2. Experimental Setup

Sample collection of PM$_{10}$ took place over 3 weeks in the 2022 spring, from the end of May to mid-June, covering one week in each dwelling. Continuous monitoring of PM$_{10}$ was performed with photometric instruments (DustTrak, DRX 8533 and Optical Particle Size, OPS 3330, both instruments from TSI Inc., Shoreview, MN, USA). Measurements of CO$_2$ were carried out with WolfSense probes (Gray Wolf®, Roswell, GA, USA, IQ-610). The real-time monitors were operated with a sampling rate of 1 min and were previously calibrated by the manufacturers before the monitoring campaign. In addition, before moving to the next house, the inlet was cleaned, the impactors greased, and the zero check was performed with a high-efficiency particulate air (HEPA) filter. Simultaneously, the gravimetric collection of PM$_{10}$ took place for 24 h and was performed by low-volume samplers (Echo Tecora, Italy and Leckel LVS6, Germany) at a constant flow rate of 2.3 m^3 h^{-1}, equipped with 47 mm pre-weighed PTFE filters (Pall).

The instrumentation set consisted of one photometric and gravimetric instrument and a CO$_2$ monitor for each microenvironment, following the same configuration in each dwelling: bedroom—OPS, Tecora, and WolfSense; living room—DustTrak, Leckel, and WolfSense; and kitchen—DustTrak, Leckel, and WolfSense. CO$_2$ was used to calculate the air change rate. In all microenvironments, the samplers were positioned at a minimum distance of 1 m from the walls and at 1.5 m height, which corresponds approximately to the breathing zone.

2.3. Data Quality Assurance

Photometric instruments can provide a high spatiotemporal resolution capable of reporting PM in real time [36–38]. However, these instruments can suffer deviations due to different responses in the measurement of various types of aerosols [39,40]. The calibration process is essential to ensure accurate measurements under the prevailing ambient

conditions. Tecora and Leckel samplers are certified by the European Committee for Standardisation as reference instruments for PM_{10} measurements according to EN 14907. In situ comparisons between photometric and gravimetric instruments showed a good reproducibility for 24 h measurements for each microenvironment: bedroom (r^2 = 0.82–0.92; slope between 0.8 and 1.1 and y-offset between −5.5 and 3); living room (r^2 = 0.84–0.99; slope between 0.7 and 2 and y-offset between −0.21 and −0.04); and kitchen (r^2 = 0.83–0.91; slope between 1.6 and 2.6 and y-offset between −4.1 and 1.8). Therefore, PM_{10} hourly concentrations of DustTrak and OPS instruments were rectified using the equations (Figure S1, Supplementary Material) obtained from the intercomparison with the reference method. The values found are in agreement with previous studies, in which it was observed that the OPS (factory calibrated with density of 1 g cm^{-3}) generally underestimates the concentrations in relation to the gravimetric method [41], while DustTraks (factory calibrated with Arizona Road Dust with a density of 2.65 g cm^{-3}) overestimate by 1.94–2.57 times filter-based concentrations [39,42,43].

2.4. Air Change Rate

To characterise the ventilation in the microenvironments, air changes per hour (ACH, h^{-1}) were calculated using the CO_2 decay method. Decay or step-down methods can be used when a space is vacated after occupancy. ACH is typically estimated by analysing how quickly CO_2 concentrations decrease in a room after the source has been stopped. More details can be found in Hänninen [44] and elsewhere. Previous studies applied the same methodology in different microenvironments, such as educational buildings [45], classrooms [46], and a university cafeteria [47].

2.5. Black Carbon Analyses

All PM_{10} samples obtained from gravimetric measurements were analysed by a Multi-wavelength Absorption Black Carbon Instrument (MABI, Ansto) to determine the BC concentrations in the filters. The light absorption was measured through unexposed filters (I_o) and exposed filters (I) at seven wavelengths (405 nm, 465 nm, 525 nm, 639 nm, 870 nm, 940 nm, and 1050 nm), and the BC mass concentrations were determined for each wavelength following Equation (1):

$$BC\left(\mu g\ m^{-3}\right) = \frac{10^2.A}{\varepsilon.V}.\ln\left[\frac{I_o}{I}\right] = \frac{b_{abs}}{\varepsilon} \tag{1}$$

The mass absorption coefficient (ε) for each wavelength (Table S1, Supplementary Material) was estimated using the central wavelength (λ = 639 nm) as a reference with a value of ε = 6.036 $m^2\ g^{-1}$, which was recommended for 47 mm Teflon filters by ANSTO [48] and Ryś et al. [49]. BC from different sources can vary in light-absorbing ability. Concentration from biomass burning is mainly associated with the lowest wavelength (405 nm), while fossil fuel emissions are related to the highest wavelength (1050 nm) [49,50]. This allows for differentiation of biomass burning contributions by subtracting $BC_{405\ nm}$–$BC_{1050\ nm}$ concentrations.

2.6. Deposition Dose and Dosimetry in the Human Respiratory Tract

PM_{10} and BC depositions in the human respiratory tract (HRT) were calculated using the Multiple-Path Particle Dosimetry model (MPPD, v 3.04). The model can provide the total and regional deposition fractions (DFs) in the HRT, namely on head (H), tracheobronchial (TB), and pulmonary (P) regions [51]. DF refers to the proportion of size-segregated particles that deposit in a specific region compared to the total mass of particles of the same size that initially enter in the HRT [52]. A constant exposure scenario considering a light activity (e.g., sitting) was set for adult males and females (25–30 years old). The physiological parameters used in the model were obtained from the International Commission on Radiological Protection (ICRP) [53], and these are given in Table 2. The Yeh-Schum 5-Lobe model was adopted, representing an asymmetric human lung with multiple paths [54].

Table 2. Input parameters in the MPPD model.

Parameters		Options/Values	
		Adult Male	Adult Female
Airway Morphometry	Species	Human	
	Model	Yeh/Schum 5-Lobe	
	FRC (mL) [a]	3300	2680
	URT volume (mL) [a]	50	40
	Density (g cm^{-3})	1	
Particle Properties	Aspect ratio	1	
	Diameter (μm)	MMAD	
	Particle distribution	Single	
	MMAD	H1 = 5.96, H2 = 4.95, H3 = 7.74	
	GSD	H1 = 2.13, H2 = 3.17, H3 = 2.82	
	Exposure condition	Constant exposure	
Exposure Scenario	Aerosol concentration (μg m^{-3})	Mean of PM$_{10}$	
	Breathing frequency (min^{-1}) [a]	12	14
	Tidal volume (mL) [a]	750	464
	Inspiratory fraction	0.5	0.5
	Breathing scenario	Nasal	

[a] Reference [53]; H1 = house 1; H2 = house 2; H3 = house 3; URT—upper respiratory tract; FRC—functional residual capacity; MMAD—mass median diameter; GSD—geometric standard deviation.

The model default particle density (1 g cm^{-3}) and a shape factor value of 1 were assumed to run the model. PM$_{10}$ mass median diameter (MMAD) and geometric standard deviation (GSD) were calculated for each dwelling using the size-segregated data obtained from the OPS (16 channels in the range from 0.3 to 10 μm). MMAD and GSD values for BC were taken as 0.3 μm and 2.92, respectively, based on the study by Hitzenberger et al. [55]. The PM$_{10}$ and BC total and regional doses were estimated using Equation (2) [56]:

$$Dose\left(\mu g\,min^{-1}\right) = C \times DF \times VE \qquad (2)$$

where C is the mean concentration of PM$_{10}$ or BC (μg m^{-3}) for each microenvironment, DF is the total or regional deposition fraction, and VE is the ventilation per minute (m^3 min^{-1}). The VE values were set to 0.009 m^3 min^{-1} and 0.0065 m^3 min^{-1} for short-term exposure of males and females, respectively [53].

2.7. Air Mass Trajectories

In the Iberian Peninsula, Saharan dust and wildfire smoke can contribute to increased PM concentrations [57–60]. To identify possible long-range transport events to the receptor sites, backward trajectories were calculated using the Hybrid Single-Particle Lagrangian Integrated Trajectory (HYSPLIT 4.0) model [61], combined with the location of fire foci (http://effis.jrc.ec.europa.eu/, accessed on 12 December 2022). In this study, 5-day backward trajectories were computed for the days with elevated concentrations (>90th percentile), using the Global Forecast System Reanalysis (0.25°, global) arriving at 1500 m above ground level. The 850 hPa pressure level (i.e., 1500 m) was selected as the characteristic height of the top of the transport layer, which is representative for this region [62].

2.8. Statistical Analyses

All descriptive statistics and tests were performed using SPSS software (IBM Statistics software v. 24) and MATLAB 2018a (The MathWorks Inc., Natick, MA, USA). PM$_{10}$ and BC concentrations were tested for normality with the Shapiro–Wilk test. The Mann–Whitney test was used to evaluate the differences between microenvironments. Pearson's correlations were employed to establish linear relationships between gravimetric and light-scattering measurements. A significance level of 5% was used for all tests ($p < 0.05$).

3. Results and Discussion

3.1. PM_{10} Concentrations

From the gravimetric determination of PM_{10}, the indoor daily concentrations of PM_{10} for all selected microenvironments are shown in Figure 2. High inter-house variations were observed. Mean concentrations of PM_{10} in house 3 considering all microenvironments (51.2 µg m^{-3}) were around 4 and 3 times higher than in house 2 (12.4 µg m^{-3}) and house 1 (17.9 µg m^{-3}), respectively. PM_{10} levels for each dwelling did not show significant statistical differences between the monitored microenvironments, except in house 2, for which notable differences ($p < 0.05$) were registered. The daily PM_{10} surpassed the threshold of 50 µg m^{-3} imposed by the European legislation (Directive 2008/50/EC) on 50% of measurement days in house 3, whilst no exceedances were observed for houses 1 and 2.
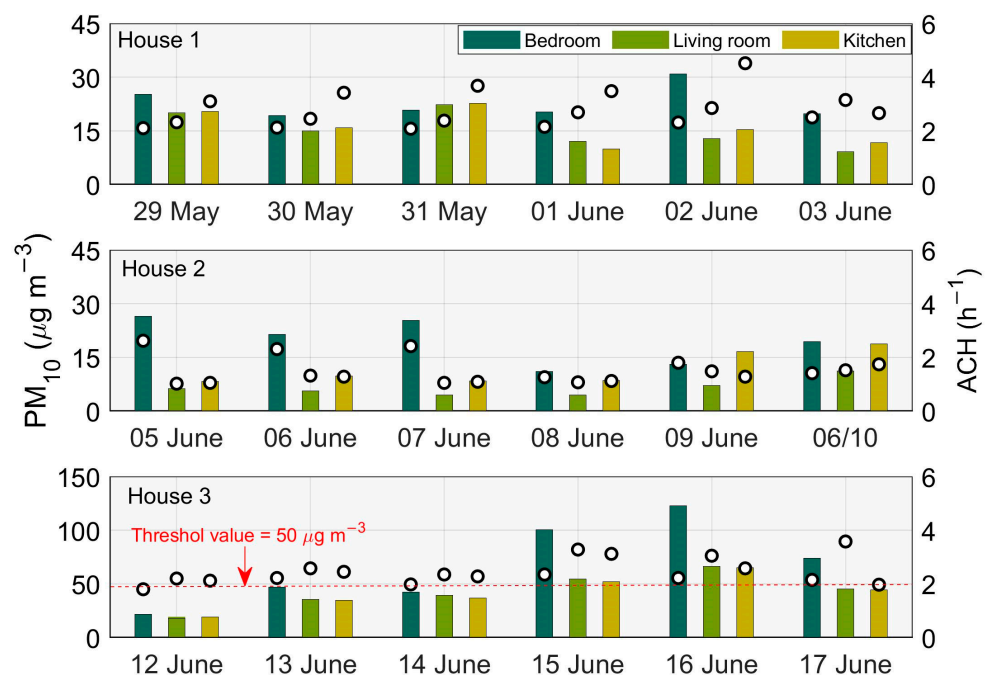

Figure 2. PM_{10} 24 h mean concentrations and ACH for the whole campaign divided by microenvironments.

The average of the ACH (h^{-1}) calculations for each microenvironment were as follows: house 1 (B—2.21; LR—2.64; K—3.41), house 2 (B—1.97; LR—1.21; K—1.26), and house 3 (B—2.12; LR—2.84; K—2.42). The information on door/window opening and closing procedures was recorded by occupants in a logbook. Records suggest that, in house 2, CDCW (closed doors, closed windows) predominated, which may have contributed to the lower ACHs and statistical differences between microenvironments. In addition, the living room of this dwelling was only accessed for a few minutes on three days of the sampling period, which may explain the low ACH and pollutant concentration values.

The ventilation setting associated with higher daily PM_{10} concentrations was closed doors with semi-open windows (CDSW), which was practised in all bedrooms (house 1—22.7 µg m^{-3}; house 2—17.5 µg m^{-3}; and house 3—68.1 µg m^{-3}). On the other hand, the lowest PM_{10} mean concentrations (LR = 6.53 µg m^{-3}; K = 11.7 µg m^{-3}) were recorded in house 2, for ventilation conditions characterised by CDCW (closed doors and windows). These results are distinct from those reported by Canha et al. [63], who studied PM_{10} concentrations for different ventilation configurations in bedrooms, reporting the highest mean concentrations for CDCW (26.7 µg m^{-3}) and the lowest for ODCW (18.5 µg m^{-3}). The lower occupancy in the LR and K of house 2 likely contributed to lower PM_{10} concentrations. In addition, the ventilation settings (e.g., CDCW) can act as a barrier against infiltration of air pollutants or migration from another microenvironment. In another study, higher PM_{10}

concentrations with increasing ACH values were registered because of the infiltration of outdoor air [30].

The hourly PM_{10} mean concentrations for the measurement days are shown in Figure 3. In bedrooms (a, d, and g), PM_{10} concentrations increased sharply between 8 and 10 a.m. and 6 and 7 p.m., corresponding to getting up and returning in the late afternoon. Due to the lower activities registered in the K and LR of the house 2, PM_{10} concentrations did not show marked variation throughout the day. On the other hand, PM_{10} concentrations in the kitchen of house 1 (c) were linked to frequent cooking activities (9–12 a.m. and 6–9 p.m.). The living room of the same house presented a very similar pattern (b), probably due to the migration of cooking fumes from the kitchen and the use of this microenvironment after meals by the occupants.
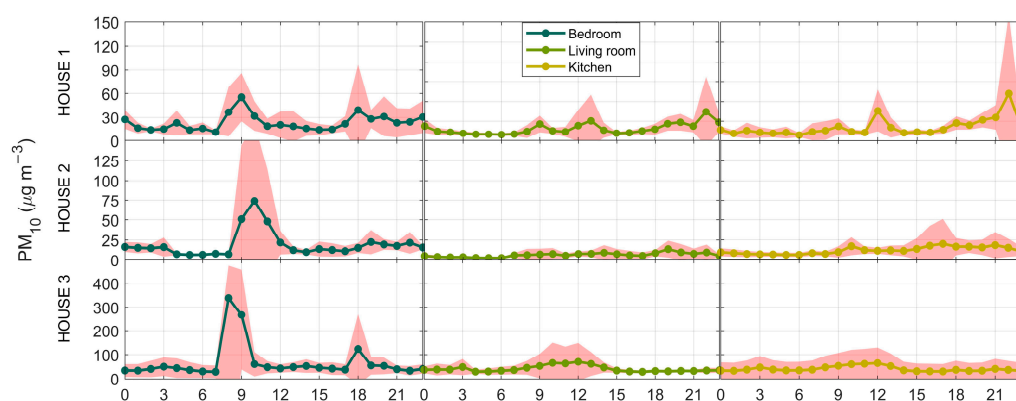

Figure 3. Diurnal cycle of PM_{10} concentrations obtained from continuous monitoring in each microenvironment: bedrooms (blue lines), the living rooms (green lines), and the kitchens (yellow lines) of houses 1, 2, and 3, respectively. Filled areas in red correspond to the associated errors.

The inspection of the diurnal cycle and the notes in the logbooks referring to the activities in the bedrooms showed that the highest peaks (house 1 = 55.3 $\mu g\ m^{-3}$ and house 3 = 339 $\mu g\ m^{-3}$) corresponded to making the beds and the use of aerosol sprays and incense. Details of the main activities can be seen in Table S2 in the Supplementary Material. In addition to indoor sources, outdoor contributions to PM levels were notable in house 3 for all microenvironments. The backward trajectories showed contributions from the long-range transport of smoke from wildfires located in Zamora (Spain) and dust from the Sahara (Africa) only for the sampling period in house 3, which is shown in Figure S2 of the Supplementary Material. Thus, indoor air pollution in house 3 represented a mixture of indoor sources and long-range transport. Furthermore, in addition to the dominant mineral matter, anthropogenic constituents such as BC can also represent a significant aerosol component during dust outbreaks. Different processes can lead to an increase in the anthropogenic PM load of the dust. Among others, these processes include anthropogenic emission sources in the proximity of the desert, such as large petrochemical and power plants, frequent wildfires in the Sub-Saharan region, and interaction between the mineral particles and anthropogenic emissions during transport [64]. Only on the 1st day (06/12), no influence of smoke and dust on indoor PM concentrations was observed. On the other hand, the concentrations recorded on the 5th day (06/15) were the highest, corresponding to 5.7-, 3.7-, and 3.4-fold increases in PM_{10} levels compared to those on the first day (06/12) for the bedroom, living room, and kitchen, respectively. Higher PM_{10} levels in the bedroom may be associated with the orientation of the window (opposite to the kitchen and living room), in addition to common housekeeping activities, which favour dust resuspension in that microenvironment. Backward trajectories were also calculated for the sampling periods in houses 1 and 2 and showed no influence of long-range transport of dust or smoke.

In house 2, the morning peak in the bedroom (74.1 $\mu g\ m^{-3}$) can be related to infiltration from the outdoors of PM from high traffic on the adjacent avenue. In fact, opening the window took place around 8 a.m., during the period of greatest road congestion [38].

Abdel-Salam et al. [65] reported stronger correlations between indoor and outdoor PM_{10} concentrations through frequent opening of ventilation settings, which favours the infiltration of pollutants from outdoor air into indoor microenvironments.

3.2. Black Carbon Concentrations

BC is emitted directly from combustion sources and is a good indicator of traffic-related PM pollution [66,67]. Higher percentages of BC in PM_{10} (between 15% and 22.6%) were found in house 2. In general, markedly higher concentrations were observed for BC in the bedrooms (Figure 4) (house 1 = 3.63 μg m^{-3}, house 2 = 2.93 μg m^{-3}, and house 3 = 5.17 μg m^{-3}), likely due to both indoor activities (candles and incense) and outdoor sources, including the infiltration of vehicular traffic emissions, given that these compartments were located on the facade of the buildings facing the main streets.
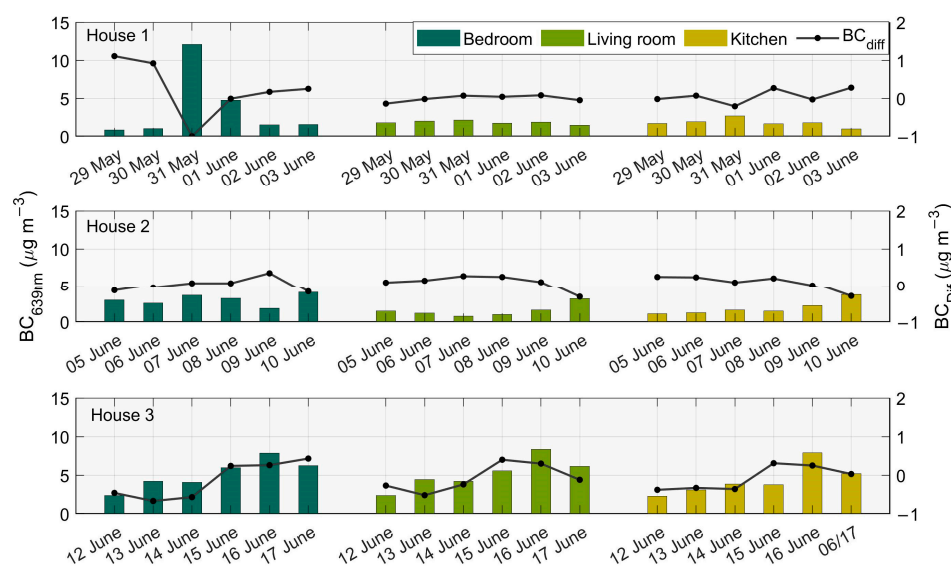

Figure 4. Black carbon concentrations for the entire campaign. BC_{diff} (right *y*-axis) represents the difference in concentrations between the lower (405 nm) and upper wavelengths (1050 nm) to characterise the contribution of biomass burning.

BC_{diff} values (black line) higher than 0.5 μg m^{-3} suggest an impact from biomass burning combined with other sources, while values close to or less than 0 represent a major contribution from vehicular emissions [50]. The highest daily values of BC_{diff} were found in the bedroom of house 1, likely due to specific indoor sources (candles and incense). However, BC concentrations in the corresponding days were low (05/29 = 0.83 μg m^{-3} and 05/30 = 1.01 μg m^{-3}). On the other hand, the highest daily BC value for all microenvironments (12.1 μg m^{-3}) was recorded in the bedroom of house 1, but no specific activities were written down in the logbook that allow explaining this concentration, suggesting infiltration from outdoor pollution from traffic. As expected, house 2 displayed BC_{diff} values close to 0 for all microenvironments, confirming the influence of traffic emissions. Substantial variations in BC concentrations in house 3 were registered. Considering the entire period, average BC contributions from fossil fuel (BC_{ff}) were higher than that from biomass burning (BC_{bb}) for all houses (house 1: BC_{ff} = 90% and BC_{bb} = 10%; house 2: BC_{ff} = 93% and BC_{bb} = 7%; and house 3: BC_{ff} = 88% and BC_{bb} = 12%). As mentioned earlier, the sampling period in this house covered a desert dust intrusion event, which contributed to increased levels of particulate material and specific chemical constituents [68].

3.3. Deposition Fractions and Dose of PM_{10} and BC

The PM_{10} and BC total and regional deposition fractions are shown in Table 3. Total PM_{10} deposition fractions ranged from 73% to 86% for males and 69% to 83% for females. In general, the regional DF of PM_{10} showed a similar pattern, irrespective of the house:

H > P > TB. On the other hand, the regional DF for BC presented higher values for the P region, followed by H and TB. In summary, given that BC is essentially bound to the finest particles, its deposition is governed by Brownian diffusion, and penetrates deeper into the airways, while PM_{10} is mainly deposited in the upper region of the HRT by mechanisms involving impact and gravitational sedimentation [69,70]. These results are in line with findings from other authors [38,71,72].

Table 3. Total and regional DF of PM_{10} and BC.

		PM_{10}			
Sites	**Gender**	**Total**	**Head**	**Tracheobronchial**	**Pulmonary**
House 1	Male	0.86	0.73	0.04	0.09
	Female	0.83	0.69	0.05	0.08
House 2	Male	0.73	0.61	0.03	0.09
	Female	0.69	0.57	0.04	0.08
House 3	Male	0.79	0.67	0.03	0.08
	Female	0.76	0.64	0.04	0.08
		BC			
All houses	Male	0.30	0.10	0.06	0.14
	Female	0.26	0.08	0.07	0.11

Regardless of gender, total DF was mainly dependent on MMAD and GSD values. However, the values of the total DF for males were slightly higher than for females, except for the TB region. The differences in total DFs between genders can be attributed to larger and heavier lungs, tidal volume, and functional residual capacity for males [73]. Higher values for males than for females have been also reported in previous studies [74,75].

Doses were estimated for both sexes and the three microenvironments based on mean PM_{10} concentrations (Figure 5). The PM_{10} regional dose showed the largest fraction in the H region: house 1 at 0.07–0.15 µg min^{-1}, house 2 at 0.02–0.11 µg min^{-1}, and house 3 at 0.17–0.45 µg min^{-1}, representing 86% of the total dose. In comparison, the doses for the P region were as follows: house 1 at 0.05–0.08×10^{-1} µg min^{-1}, house 2 at 0.02–0.05×10^{-1} µg min^{-1}, and house 3 at 0.1–0.2×10^{-1} µg min^{-1}. The does for the TB region were as follows: house 1 at 0.08–0.18×10^{-1} µg min^{-1}, house 2 at 0.03–0.15×10^{-1} µg min^{-1}, and house 3 at 0.22–0.50×10^{-1} µg min^{-1}. Similar PM_{10} doses for the upper region were reported in a previous study, with contributions up to 99% in the H region [76]. The doses of PM_{10} followed the trend observed for the DF, with higher values for males compared to females. Furthermore, regarding the specific microenvironments, the following order was observed for the dose of PM_{10}: house 3 (B > LR > K) > house 1 (B > K > LR) > house 2 (B > K > LR).

Unlike PM_{10}, BC inhaled in different microenvironments showed the same pattern, with higher contributions to the P region: house 1 at 1.8–4.6×10^{-3} µg min^{-1}, house 2 at 1.5–3.7×10^{-3} µg min^{-1}, and house 3 at 4.5–6.6×10^{-3} µg min^{-1}. This was followed by the H region: house 1 at 1.4–3.2×10^{-3} µg min^{-1}, house 2 at 1.2–2.6×10^{-3} µg min^{-1}, and house 3 at 3.4–4.5×10^{-3} µg min^{-1}. This was then followed by the TB region: house 1 at 1.0–2.1×10^{-3} µg min^{-1}, house 2 at 0.8–1.7×10^{-3} µg min^{-1}, and house 3 at 2.5–2.9×10^{-3} µg min^{-1}. Doses in the P region accounted for up to 45% of the total doses. These results highlight the deposition of finer particles, in particular BC, in the pulmonary region. Several studies have shown increased harm to human health with decreasing particle sizes [77]. BC deposition in the P region is responsible for severe respiratory health problems due to the induction of mutagenicity, intracellular oxidative stress, and inflammatory responses [78,79].
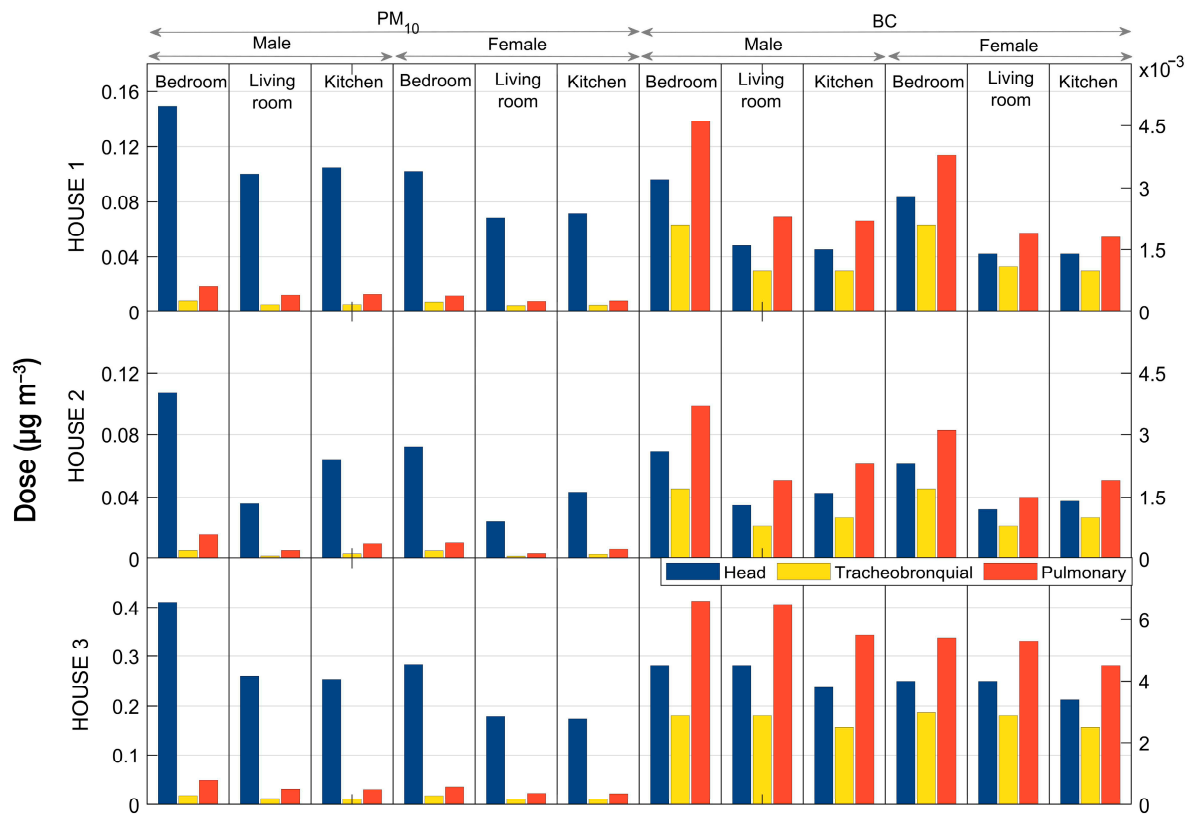
Figure 5. Regional (head, tracheobronchial, and pulmonary) dose (µg min^{-1}) of PM$_{10}$ and BC for each microenvironment, split per dwelling and gender.

3.4. Study Limitations

Some limitations to the study carried out can be pointed out, which may partially influence the interpretations made: (i) lack of monitoring of pollutants outside homes, to better understand the contribution and infiltration from outdoor sources; (ii) the limited number of houses covered in the study; (iii) size-segregated PM monitors available only in the bedrooms (OPS); (iv) calculations of PM$_{10}$ and BC deposition in the HRT performed with lung parameters and MMAD and GSD values for BC from the literature and model calculations only apply to adult males and females (25–30 years old). Hence, future studies should cover different seasons and simultaneous monitoring inside and outside, including monitors that provide size-segregated PM and BC concentrations. In addition, more houses should be considered in other urban areas, with other sources and pollution loads.

4. Conclusions

The monitoring of air pollutants in homes is usually carried out in only one specific microenvironment. This study demonstrated that the exposure assessment can be biased, as concentrations can vary from compartment to compartment. The specific ventilation conditions, together with the different activities by the occupants, were determinant for the significant differences in PM and BC concentrations. Increasing the air change rate by opening ventilation settings can improve PM dispersion. However, it can also result in the infiltration of certain pollutants from sources other than those present in the microenvironment.

In this study, which covered houses essentially occupied by students, it was found that the hotspot for exposure to PM$_{10}$ and BC concentrations is the bedroom microenvironment. Furthermore, the MPPD model indicated that the highest deposition doses occur in this hotspot, pointing to higher total deposition fractions of PM$_{10}$ in the head region, while BC is mainly deposited in the pulmonary region. It has been observed that finer particles can penetrate deeper into the HRT, potentially causing adverse health effects, especially for

males, who inhale higher total doses than females. As future work, a detailed chemical characterisation of indoor and outdoor pollutants is recommended, including not only size-segregated particles, but also gases, for a more complete picture of the impact of domestic activities and specific events on concentrations and exposure.

Supplementary Materials: The following supporting information can be downloaded at: https://www.mdpi.com/article/10.3390/atmos14071064/s1. Figure S1. Linear correlation between PM_{10} concentrations obtained from photometric and gravimetric devices for each microenvironment during the sampling campaign; Table S1. Absorption coefficients (ε) for each wavelength by microenvironment using λ = 639 nm as baseline; Figure S2. Five-day backward trajectories arriving at house 3 at 6 p.m. on five different days. Figure S3. Daily profile of CO_2 concentrations and activities associated with each peak.

Author Contributions: Conceptualisation, Y.A.C. and C.A.; methodology, Y.A.C., C.A., C.A.G. and S.M.A.; data curation, Y.A.C.; visualisation, Y.A.C.; writing—original draft preparation, Y.A.C. and C.A.; writing—review and editing, Y.A.C., C.A. and S.M.A.; supervision, C.A. and M.F.; funding acquisition, C.A. and M.F. All authors have read and agreed to the published version of the manuscript.

Institutional Review Board Statement: Not applicable.

Informed Consent Statement: Not applicable.

Data Availability Statement: The data presented in this study are available upon request from the corresponding author.

Conflicts of Interest: The authors declare no conflict of interest.

References

1. Saini, J.; Dutta, M.; Marques, G. A Comprehensive Review on Indoor Air Quality Monitoring Systems for Enhanced Public Health. *Sustain. Environ. Res.* **2020**, *30*, 6. [CrossRef]
2. Van Tran, V.; Park, D.; Lee, Y.C. Indoor Air Pollution, Related Human Diseases, and Recent Trends in the Control and Improvement of Indoor Air Quality. *Int. J. Environ. Res. Public Health* **2020**, *17*, 2927. [CrossRef] [PubMed]
3. Cincinelli, A.; Martellini, T. Indoor Air Quality and Health. *Int. J. Environ. Res. Public Health* **2017**, *14*, 1286. [CrossRef]
4. Landrigan, P.J.; Fuller, R.; Acosta, N.J.R.; Adeyi, O.; Arnold, R.; Basu, N.; Baldé, A.B.; Bertollini, R.; Bose-O'Reilly, S.; Boufford, J.I.; et al. The Lancet Commission on Pollution and Health. *Lancet* **2018**, *391*, 462–512. [CrossRef] [PubMed]
5. World Health Organization. *Health, Environment and Climate Change: Report by the Director-General*; World Health Organization: Geneva, Switzerland, 2018; Available online: https://apps.who.int/iris/handle/10665/276332 (accessed on 24 May 2023).
6. Lange, P.; Celli, B.; Agustí, A.; Boje Jensen, G.; Divo, M.; Faner, R.; Guerra, S.; Marott, J.L.; Martinez, F.D.; Martinez-Camblor, P.; et al. Lung-Function Trajectories Leading to Chronic Obstructive Pulmonary Disease. *N. Engl. J. Med.* **2015**, *373*, 111–122. [CrossRef] [PubMed]
7. Liu, S.; Zhou, Y.; Liu, S.; Chen, X.; Zou, W.; Zhao, D.; Li, X.; Pu, J.; Huang, L.; Chen, J.; et al. Association between Exposure to Ambient Particulate Matter and Chronic Obstructive Pulmonary Disease: Results from a Cross-Sectional Study in China. *Thorax* **2017**, *72*, 788–795. [CrossRef]
8. Farraj, A.K.; Walsh, L.; Haykal-Coates, N.; Malik, F.; Mcgee, J.; Winsett, D.; Duvall, R.; Kovalcik, K.; Cascio, W.E.; Higuchi, M.; et al. Carbon Black Nanoparticle Instillation Induces Sustained Inflammation and Genotoxicity in Mouse Lung and Liver. *Part. Fibre Toxicol.* **2012**, *9*, 5. [CrossRef]
9. Brook, R.D.; Rajagopalan, S.; Pope, C.A.; Brook, J.R.; Bhatnagar, A.; Diez-Roux, A.V.; Holguin, F.; Hong, Y.; Luepker, R.V.; Mittleman, M.A.; et al. Particulate Matter Air Pollution and Cardiovascular Disease. *Circulation* **2010**, *121*, 2331–2378. [CrossRef]
10. Gray, D.L.; Wallace, L.A.; Brinkman, M.C.; Buehler, S.S.; La Londe, C. Respiratory and Cardiovascular Effects of Metals in Ambient Particulate Matter: A Critical Review. *Rev. Environ. Contam. Toxicol.* **2015**, *234*, 135–203. [CrossRef]
11. World Health Organization. Household Air Pollution. 2022. Available online: https://www.who.int/news-room/fact-sheets/detail/household-air-pollution-and-health (accessed on 30 March 2023).

12. Loomis, D.; Grosse, Y.; Lauby-Secretan, B.; El Ghissassi, F.; Bouvard, V.; Benbrahim-Tallaa, L.; Guha, N.; Baan, R.; Mattock, H.; Straif, K. The Carcinogenicity of Outdoor Air Pollution. *Lancet Oncol.* **2013**, *14*, 1262. [CrossRef]

13. Cohen, A.J.; Brauer, M.; Burnett, R.; Anderson, H.R.; Frostad, J.; Estep, K.; Balakrishnan, K.; Brunekreef, B.; Dandona, L.; Dandona, R.; et al. Estimates and 25-Year Trends of the Global Burden of Disease Attributable to Ambient Air Pollution: An Analysis of Data from the Global Burden of Diseases Study 2015. *Lancet* **2017**, *389*, 1907–1918. [CrossRef] [PubMed]

14. Seinfeld, J.H.; Pandis, S.N. *Atmospheric Chemistry and Physics: From Air Pollution to Climate Change*; John Wiley & Sons: New York, NY, USA, 2016.

15. Leech, J.A.; Nelson, W.C.; Burnett, R.T.; Aaron, S.; Raizenne, M.E. It's about Time: A Comparison of Canadian and American Time–Activity Patterns. *J. Expo. Sci. Environ. Epidemiol.* **2002**, *12*, 427–432. [CrossRef] [PubMed]

16. Han, Y.; Li, X.; Zhu, T.; Lv, D.; Chen, Y.; Hou, L.A.; Zhang, Y.; Ren, M. Characteristics and Relationships between Indoor and Outdoor $PM_{2.5}$ in Beijing: A Residential Apartment Case Study. *Aerosol Air Qual. Res.* **2016**, *16*, 2386–2395. [CrossRef]

17. Gao, X.; Gao, W.; Sun, X.; Jiang, W.; Wang, Z.; Li, W. Measurements of Indoor and Outdoor Fine Particulate Matter during the Heating Period in Jinan, in North China: Chemical Composition, Health Risk, and Source Apportionment. *Atmosphere* **2020**, *11*, 885. [CrossRef]

18. Tofful, L.; Perrino, C.; Canepari, S. Comparison Study between Indoor and Outdoor Chemical Composition of $PM_{2.5}$ in Two Italian Areas. *Atmosphere* **2020**, *11*, 368. [CrossRef]

19. Alves, C.; Vicente, A.; Oliveira, A.R.; Candeias, C.; Vicente, E.; Nunes, T.; Cerqueira, M.; Evtyugina, M.; Rocha, F.; Almeida, S.M. Fine Particulate Matter and Gaseous Compounds in Kitchens and Outdoor Air of Different Dwellings. *Int. J. Environ. Res. Public Health* **2020**, *17*, 5256. [CrossRef]

20. Canha, N.; Lage, J.; Galinha, C.; Coentro, S.; Alves, C.; Almeida, S.M. Impact of Biomass Home Heating, Cooking Styles, and Bread Toasting on the Indoor Air Quality at Portuguese Dwellings: A Case Study. *Atmosphere* **2018**, *9*, 214. [CrossRef]

21. Pastuszka, J.S.; Talik, E.; Płoszaj-Pyrek, J.; Grygierek, K.; Ferdyn-Grygierek, J. Exposure to PM_4 in Homes with Tobacco Smoke in and around Katowice, Poland. *Atmosphere* **2021**, *12*, 1590. [CrossRef]

22. Vicente, E.D.; Alves, C.A.; Martins, V.; Almeida, S.M.; Lazaridis, M. Lung-Deposited Dose of Particulate Matter from Residential Exposure to Smoke from Wood Burning. *Environ. Sci. Pollut. Res.* **2021**, *28*, 65385–65398. [CrossRef]

23. Qian, J.; Peccia, J.; Ferro, A.R. Walking-Induced Particle Resuspension in Indoor Environments. *Atmos. Environ.* **2014**, *89*, 464–481. [CrossRef]

24. Karagulian, F.; Belis, C.A.; Dora, C.F.C.; Prüss-Ustün, A.M.; Bonjour, S.; Adair-Rohani, H.; Amann, M. Contributions to Cities' Ambient Particulate Matter (PM): A Systematic Review of Local Source Contributions at Global Level. *Atmos. Environ.* **2015**, *120*, 475–483. [CrossRef]

25. Vardoulakis, S.; Dimitrova, R.; Richards, K.; Hamlyn, D.; Camilleri, G.; Weeks, M.; Sini, J.F.; Britter, R.; Borrego, C.; Schatzmann, M.; et al. Numerical Model Inter-Comparison for Wind Flow and Turbulence Around Single-Block Buildings. *Environ. Model. Assess.* **2011**, *16*, 169–181. [CrossRef]

26. Nadali, A.; Arfaeinia, H.; Asadgol, Z.; Fahiminia, M. Indoor and Outdoor Concentration of PM_{10}, $PM_{2.5}$ and PM_1 in Residential Building and Evaluation of Negative Air Ions (NAIs) in Indoor PM Removal. *Environ. Pollut. Bioavailab.* **2020**, *32*, 47–55. [CrossRef]

27. Yang, Y.Y.; Fan, L.; Wang, J.; Zhu, Y.D.; Li, X.; Wang, X.Q.; Yan, X.; Li, L.; Zhang, Y.; Yang, W.; et al. Characterization and Exposure Assessment of Household Fine Particulate Matter Pollution in China. *Indoor Air* **2021**, *31*, 1391–1401. [CrossRef]

28. Feliciano, M.; Lira, F.; Furst, L.C.; Arioli, R. The influence of domestic heating systems in indoor air quality in homes of a region of Northeastern Portugal. *Prog. Ind. Ecol.* **2022**, *15*, 162–182. [CrossRef]

29. BéruBé, K.A.; Sexton, K.J.; Jones, T.P.; Moreno, T.; Anderson, S.; Richards, R.J. The Spatial and Temporal Variations in PM_{10} Mass from Six UK Homes. *Sci. Total Environ.* **2004**, *324*, 41–53. [CrossRef]

30. Abdel-Salam, M.M.M. Indoor Exposure of Elderly to Air Pollutants in Residential Buildings in Alexandria, Egypt. *Build. Environ.* **2022**, *219*, 109221. [CrossRef]

31. Scibor, M. Are We Safe inside? Indoor Air Quality in Relation to Outdoor Concentration of PM_{10} and $PM_{2.5}$ and to Characteristics of Homes. *Sustain. Cities Soc.* **2019**, *48*, 101537. [CrossRef]

32. Madureira, J.; Slezakova, K.; Silva, A.I.; Lage, B.; Mendes, A.; Aguiar, L.; Pereira, M.C.; Teixeira, J.P.; Costa, C. Assessment of Indoor Air Exposure at Residential Homes: Inhalation Dose and Lung Deposition of PM_{10}, $PM_{2.5}$ and Ultrafine Particles among Newborn Children and Their Mothers. *Sci. Total Environ.* **2020**, *717*, 137293. [CrossRef]

33. Pordata. Municipalities Database. Available online: https://www.pordata.pt/Municipios (accessed on 21 March 2023).

34. Peel, M.C.; Finlayson, B.L.; Mcmahon, T.A. Hydrology and Earth System Sciences Updated World Map of the Köppen-Geiger Climate Classification. *Hydrol. Earth Syst. Sci* **2007**, *11*, 1633–1644. [CrossRef]

35. Gonçalves, A.; Ornellas, G.; Ribeiro, A.C.; Maia, F.; Rocha, A.; Feliciano, M. Urban Cold and Heat Island in the City of Bragança (Portugal). *Climate* **2018**, *6*, 70. [CrossRef]

36. Carrico, C.M.; Karacaoglu, J. Impacts of a Prescribed Fire on Air Quality in Central New Mexico. *Atmosphere* **2023**, *14*, 316. [CrossRef]

37. Wadlow, I.; Paton-Walsh, C.; Forehead, H.; Perez, P.; Amirghasemi, M.; Guérette, É.-A.; Gendek, O.; Kumar, P. Understanding Spatial Variability of Air Quality in Sydney: Part 2—A Roadside Case Study. *Atmosphere* **2019**, *10*, 217. [CrossRef]

38. Cipoli, Y.A.; Targino, A.C.; Krecl, P.; Furst, L.C.; dos Alves, C.A.; Feliciano, M. Ambient Concentrations and Dosimetry of Inhaled Size-Segregated Particulate Matter during Periods of Low Urban Mobility in Bragança, Portugal. *Atmos. Pollut. Res.* **2022**, *13*, 101512. [CrossRef] [PubMed]

39. Ramachandran, S.; Cherian, R. Regional and Seasonal Variations in Aerosol Optical Characteristics and Their Frequency Distributions over India during 2001–2005. *J. Geophys. Res. Atmos.* **2008**, *113*, 8207. [CrossRef]

40. Moosmüller, H.; Arnott, W.P.; Rogers, C.F.; Bowen, J.L.; Gillies, J.A.; Pierson, W.R.; Collins, J.F.; Durbin, T.D.; Norbeck, J.M. Time Resolved Charaterization of Diesel Particulate Emissions. 1. Instruments for Particle Mass Measurements. *Environ. Sci. Technol.* **2001**, *35*, 781–787. [CrossRef]

41. Raparthi, N.; Debbarma, S.; Phuleria, H.C. Development of Real-World Emission Factors for on-Road Vehicles from Motorway Tunnel Measurements. *Atmos. Environ. X* **2021**, *10*, 100113. [CrossRef]

42. Wallace, L.A.; Wheeler, A.J.; Kearney, J.; Van Ryswyk, K.; You, H.; Kulka, R.H.; Rasmussen, P.E.; Brook, J.R.; Xu, X. Validation of Continuous Particle Monitors for Personal, Indoor, and Outdoor Exposures. *J. Expo. Sci. Environ. Epidemiol.* **2010**, *21*, 49–64. [CrossRef]

43. Kingham, S.; Durand, M.; Aberkane, T.; Harrison, J.; Gaines Wilson, J.; Epton, M. Winter Comparison of TEOM, MiniVol and DustTrak PM_{10} Monitors in a Woodsmoke Environment. *Atmos. Environ.* **2006**, *40*, 338–347. [CrossRef]

44. Hänninen, O. Novel Second-Degree Solution to Single Zone Mass-Balance Equation Improves the Use of Build-up Data in Estimating Ventilation Rates in Classrooms. *J. Chem. Health Saf.* **2013**, *20*, 14–19. [CrossRef]

45. Aguilar, A.J.; de la Hoz-Torres, M.L.; Costa, N.; Arezes, P.; Martínez-Aires, M.D.; Ruiz, D.P. Assessment of Ventilation Rates inside Educational Buildings in Southwestern Europe: Analysis of Implemented Strategic Measures. *J. Build. Eng.* **2022**, *51*, 104204. [CrossRef]

46. Westgate, S.; Ng, N.L. Using In-Situ CO_2, PM_1, $PM_{2.5}$, and PM_{10} Measurements to Assess Air Change Rates and Indoor Aerosol Dynamics. *Build. Environ.* **2022**, *224*, 109559. [CrossRef]

47. Alves, C.A.; Vicente, E.D.; Evtyugina, M.; Vicente, A.M.; Nunes, T.; Lucarelli, F.; Calzolai, G.; Nava, S.; Calvo, A.I.; del Alegre, C.B.; et al. Indoor and Outdoor Air Quality: A University Cafeteria as a Case Study. *Atmos. Pollut. Res.* **2020**, *11*, 531–544. [CrossRef]

48. Atanacio, A.J.; Cohen, D.D.; Button, D.; Paneras, N.; Garton, D. Multi-Wavelength Absorption Black Carbon Instrument (MABI) Manual. Available online: https://www.ansto.gov.au/media/2716/download (accessed on 20 March 2023).

49. Ryś, A.; Samek, L. Measurement report: Determination of Black Carbon concentration in $PM_{2.5}$ fraction by Multi-wavelength absorption black carbon instrument (MABI). *Atmos. Chem. Phys.* **2021**, 1–14. [CrossRef]

50. Manohar, M.; Atanacio, A.; Button, D.; Cohen, D. MABI—A Multi-Wavelength Absorption Black Carbon Instrument for the Measurement of Fine Light Absorbing Carbon Particles. *Atmos. Pollut. Res.* **2021**, *12*, 133–140. [CrossRef]

51. Anjilvel, S. A Multiple-Path Model of Particle Deposition in the Rat Lung. *Fundam. Appl. Toxicol.* **1995**, *28*, 41–50. [CrossRef]

52. Cheng, K.H.; Swift, D.L. Calculation of Total Deposition Fraction of Ultrafine Aerosols in Human Extrathoracic and Intrathoracic Regions. *Aerosol Sci. Technol.* **1995**, *22*, 194–201. [CrossRef]

53. ICRP. Human Respiratory Tract Model for Radiological Protection. *J. Radiol. Prot.* **1994**, *66*, 24.

54. Yeh, H.; Schum, G. Models of Human Lung Airways and Their Application to Inhaled Particle Deposition. *Bull. Math. Biol.* **1980**, *42*, 461–480. [CrossRef]

55. Hitzenberger, R.; Tohno, S. Comparison of Black Carbon (BC) Aerosols in Two Urban Areas—Concentrations and Size Distributions. *Atmos. Environ.* **2001**, *35*, 2153–2167. [CrossRef]

56. Goel, A.; Izhar, S.; Gupta, T. Study of Environmental Particle Levels, Its Effects on Lung Deposition and Relationship With Human Behaviour. *Energy Environ. Sustain.* **2018**, 77–91. [CrossRef]

57. Díaz, J.; Linares, C.; Carmona, R.; Russo, A.; Ortiz, C.; Salvador, P.; Trigo, R.M. Saharan Dust Intrusions in Spain: Health Impacts and Associated Synoptic Conditions. *Environ. Res.* **2017**, *156*, 455–467. [CrossRef] [PubMed]

58. Calheiros, T.; Nunes, J.P.; Pereira, M.G. Recent Evolution of Spatial and Temporal Patterns of Burnt Areas and Fire Weather Risk in the Iberian Peninsula. *Agric. For. Meteorol.* **2020**, *287*, 107923. [CrossRef]

59. Cavaleiro, R.; Russo, A.; Sousa, P.M.; Durão, R. Association between Prevailing Circulation Patterns and Coarse Particles in Portugal. *Atmosphere* **2021**, *12*, 85. [CrossRef]

60. Nicolae, V.; Talianu, C.; Andrei, S.; Antonescu, B.; Ene, D.; Nicolae, D.; Dandocsi, A.; Toader, V.E.; Ștefan, S.; Savu, T.; et al. Multiyear Typology of Long-Range Transported Aerosols over Europe. *Atmosphere* **2019**, *10*, 482. [CrossRef]

61. Rolph, G.; Stein, A.; Stunder, B. Real-Time Environmental Applications and Display SYstem: READY. *Environ. Model. Softw.* **2017**, *95*, 210–228. [CrossRef]

62. Katsoulis, B.D. The Potential for Long-Range Transport of Air-Pollutants into Greece: A Climatological Analysis. *Sci. Total Environ.* **1999**, *231*, 101–113. [CrossRef] [PubMed]

63. Canha, N.; Lage, J.; Candeias, S.; Alves, C.; Almeida, S.M. Indoor Air Quality during Sleep under Different Ventilation Patterns. *Atmos. Pollut. Res.* **2017**, *8*, 1132–1142. [CrossRef]

64. Querol, X.; Tobías, A.; Pérez, N.; Karanasiou, A.; Amato, F.; Stafoggia, M.; Pérez García-Pando, C.; Ginoux, P.; Forastiere, F.; Gumy, S.; et al. Monitoring the Impact of Desert Dust Outbreaks for Air Quality for Health Studies. *Environ. Int.* **2019**, *130*, 104867. [CrossRef]

65. Abdel-Salam, M.M.M. Seasonal Variation in Indoor Concentrations of Air Pollutants in Residential Buildings. *J. Air Waste Manag. Assoc.* **2021**, *71*, 761–777. [CrossRef]

66. Popovicheva, O.; Chichaeva, M.; Kovach, R.; Zhdanova, E.; Kasimov, N. Seasonal, Weekly, and Diurnal Black Carbon in Moscow Megacity Background under Impact of Urban and Regional Sources. *Atmosphere* **2022**, *13*, 563. [CrossRef]
67. Reddington, C.L.; McMeeking, G.; Mann, G.W.; Coe, H.; Frontoso, M.G.; Liu, D.; Flynn, M.; Spracklen, D.V.; Carslaw, K.S. The Mass and Number Size Distributions of Black Carbon Aerosol over Europe. *Atmos. Chem. Phys.* **2013**, *13*, 4917–4939. [CrossRef]
68. Lucarelli, F.; Calzolai, G.; Chiari, M.; Nava, S.; Carraresi, L. Study of Atmospheric Aerosols by IBA Techniques: The LABEC Experience. *Nucl. Instrum. Methods Phys. Res. Sect. B Beam Interact. Mater. Atoms* **2018**, *417*, 121–127. [CrossRef]
69. Heyder, J.; Gebhart, J.; Rudolf, G.; Stahlhofen, W. Physical Factors Determining Particle Deposition in the Human Respiratory Tract. *J. Aerosol Sci.* **1980**, *11*, 505–515. [CrossRef]
70. Heyder, J.; Gebhart, J.; Rudolf, G.; Schiller, C.F.; Stahlhofen, W. Deposition of Particles in the Human Respiratory Tract in the Size Range 0.005–15 Mm. *J. Aerosol Sci.* **1986**, *17*, 811–825. [CrossRef]
71. Amoatey, P.; Omidvarborna, H.; Al-Jabri, K.; Al-Harthy, I.; Baawain, M.S.; Al-Mamun, A. Deposition Modeling of Airborne Particulate Matter on Human Respiratory Tract during Winter Seasons in Arid-Urban Environment. *Aerosol Sci. Eng.* **2022**, *6*, 71–85. [CrossRef]
72. Manojkumar, N.; Srimuruganandam, B. Age-Specific and Seasonal Deposition of Outdoor and Indoor Particulate Matter in Human Respiratory Tract. *Atmos. Pollut. Res.* **2022**, *13*, 101298. [CrossRef]
73. Carey, M.A.; Card, J.W.; Voltz, J.W.; Arbes, S.J.; Germolec, D.R.; Korach, K.S.; Zeldin, D.C. It's All about Sex: Gender, Lung Development and Lung Disease. *Trends Endocrinol. Metab.* **2007**, *18*, 308–313. [CrossRef]
74. Qiu, Z.; Song, J.; Xu, X.; Luo, Y.; Zhao, R.; Zhou, W.; Xiang, B.; Hao, Y. Commuter Exposure to Particulate Matter for Different Transportation Modes in Xi'an, China. *Atmos. Pollut. Res.* **2017**, *8*, 940–948. [CrossRef]
75. Lv, H.; Li, H.; Qiu, Z.; Zhang, F.; Song, J. Assessment of Pedestrian Exposure and Deposition of PM$_{10}$, PM$_{2.5}$ and Ultrafine Particles at an Urban Roadside: A Case Study of Xi'an, China. *Atmos. Pollut. Res.* **2021**, *12*, 112–121. [CrossRef]
76. Qiu, Z.; Wang, X.; Liu, Z.; Luo, J. Quantitative Assessment of Cyclists' Exposure to PM and BC on Different Bike Lanes. *Atmos. Pollut. Res.* **2022**, *13*, 101588. [CrossRef]
77. Islam, M.S.; Saha, S.C.; Sauret, E.; Gemci, T.; Gu, Y.T. Pulmonary Aerosol Transport and Deposition Analysis in Upper 17 Generations of the Human Respiratory Tract. *J. Aerosol Sci.* **2017**, *108*, 29–43. [CrossRef]
78. Feng, S.; Gao, D.; Liao, F.; Zhou, F.; Wang, X. The Health Effects of Ambient PM$_{2.5}$ and Potential Mechanisms. *Ecotoxicol. Environ. Saf.* **2016**, *128*, 67–74. [CrossRef]
79. Redaelli, M.; Sanchez, M.; Fuertes, E.; Blanchard, M.; Mullot, J.; Baeza-Squiban, A.; Garçon, G.; Léger, C.; Jacquemin, B. Health Effects of Ambient Black Carbon and Ultrafine Particles. *Environ. Epidemiol.* **2019**, *3*, 347–348. [CrossRef]